ORIGINAL ARTICLE

Rheological study on lower critical solution temperature behavior of organo-soluble cyano-substituted *p*-aramid in isotropic phase

Hyo Jeong Kim[1] · Yeamsuksawat Thanakorn[1] · Dae Eon Jung[2] · Youngho Eom[1]

Abstract

Poly(2-cyano-*p*-phenylene terephthalamide) (CY-PPTA) has garnered significant interest as a promising precursor for super *p*-aramid fibers because of its organosolubility in *N,N*-dimethyl acetamide/lithium chloride (DMAc/LiCl) while conserving the superior properties of the resultant fibers. However, CY-PPTA has been reported to exhibit abnormal phase behavior owing to the strong dipole–dipole interactions induced by the cyano groups. Herein, we rheologically study the isotropic phases of CY-PPTA/DMAc solutions with respect to the concentration and temperature and compare them with those of CY-PPTA/sulfuric acid (H_2SO_4) solutions. In the isotropic region, the CY-PPTA solutions yield a higher power-law exponent of the dynamic viscosity (η') versus concentration of 6.0 ($\eta' \sim c^{6.0}$) in the DMAc system than that in H_2SO_4 ($\eta' \sim c^{3.2}$). Moreover, the CY-PPTA/DMAc solutions exhibit a lower critical solution temperature (LCST) behavior with increasing temperature, in contrast with the upper critical solution temperature in H_2SO_4. Consequently, the viscosity and exponent of the CY-PPTA/DMAc solutions increase at elevated temperatures. As shown by the Cole–Cole plot, the heterogeneity in the DMAc system becomes worse. The LCST of the CY-PPTA solution is ascribed to the intermolecular interactions between the highly polar cyano groups, which are negligible in H_2SO_4.

Keywords Poly(2-cyano-*p*-phenylene terephthalamide) · Lower critical solution temperature · Isotropic phase

1 Introduction

The lyotropic phase behavior of liquid crystalline (LC) polymers has been conventionally studied using optics because it is one of the easiest and fastest methods to estimate the onset of molecular orientation and sometimes to characterize the type of molecular ordering pattern [1–3]. However, optical methods have clear drawbacks. Only molecular aggregation that is large enough to cause scattering of visible light can be observed. This, in turn, means that micro- or nano-sized associates of polymer molecules smaller than 100 nm are

undetectable in optical analysis. Nevertheless, numerous scientists and engineers regard the critical concentration (c^*) that yields the first appearance of an LC texture as the concentration at which molecular aggregation begins [4–7]. The c^* is, in fact, the concentration at which the domain size of the internal associates becomes larger than the wavelength of visible light.

In the solution of polar polymers in polar solvents, polymer molecules frequently make preferred associates in the form of a group of polar functional groups or micro-sized aggregation of the molecules, but the solution remains transparent [8, 9]. These types of microaggregates would also be present in the isotropic phase of lyotropic LC polymers, even before generating LC domains beyond c^*. When characterizing the microheterogeneity of a system invisible in optics, rheology provides more valuable information than optics because the presence of heterogeneous structures leads to changes in the rheological properties. For instance, Aharoni [10] carried out a systematic work tracing the plot shape of viscosity versus concentration, the so-called c^* curve, and found that, in some LC systems of polydisperse polymers, a shoulder peak was observed on the low-concentration side

---

Hyo Jeong Kim, Thanakorn Yeamsuksawat and Dae Eon Jung have equally contributed to the work.

✉ Youngho Eom
 eomyh@pknu.ac.kr

[1] Department of Polymer Engineering, Pukyong National University, 45 Yongso-ro, Nam-gu, Busan 48513, Republic of Korea

[2] Department of Polymer Science and Engineering, University of Massachusetts, 120 Governors Drive, Amherst, MA 01003, USA

of the c^* curve. This shoulder behavior is not observed when the optically isotropic solution is completely homogeneous over the entire concentration range below c^*. Aharoni attributed the reduced slope at the shoulder zone to the earlier formation of LC domains by high-molecular-weight polymer molecules. In other words, shoulder behavior was ascribed solely to the effects of polydispersity. It is worth mentioning, however, that the theoretical prediction of Doi showed that the viscosity of rod-like polymers increased linearly up to c^* with a constant slope of three without giving a shoulder peak [11]. In deriving this equation, Doi assumed no specific intermolecular interactions. Thus, intermolecular interactions are related to the shoulder behavior in polar polymer solutions. Unfortunately, the effects of intermolecular interactions on the shoulder behavior have received little attention.

In this study, the solution behavior of organosoluble poly(2-cyano-p-phenylene terephthalamide) (CY-PPTA) was investigated based on dynamic rheology. We found that the organosoluble p-aramid, including polar cyano groups, exhibited shoulder behavior below the c^* curve, similar to Aharoni's observation. Furthermore, shoulder behavior was observed only in the organic solvent system, N,N′-dimethyl acetamide/lithium chloride (DMAc/LiCl), and was negligible in sulfuric acid (H_2SO_4), suggesting the dependence of shoulder behavior on the solvent system. In addition, although CY-PPTA exhibited upper critical solution temperature (UCST) behavior in H_2SO_4, it exhibited lower critical solution temperature (LCST) behavior in DMAc/LiCl. A previous study by our group reported that the strong dipole–dipole interaction between cyano groups results in unusual liquid crystalline behavior by producing cholesteric ordering [12, 13]. In this regard, the unusual LCST behavior

of CY-PPTA in the DMAc/LiCl system can be ascribed to the intermolecular interactions induced by the cyano groups. Thus, this study aims to elucidate the origin of the abnormal LCST behavior of CY-PPTA solutions in the isotropic phase below c^*.

2 Experimental

2.1 Materials

Extrapure DMAc and LiCl were purchased from Daejung Co. (South Korea) and Sigma-Aldrich Co. (USA), respectively. 100% H_2SO_4 was purchased from Merck Millipore (Germany) and used as received. LiCl was activated at 300 °C for 30 min before preparing a mixed solvent of DMAc and LiCl, which had a LiCl content of 5 wt%. CY-PPTA was synthesized by the polycondensation of terephthaloyl dichloride (TPC) and 2-cyano-1,4-phenylenediamine (CY-PPD). CY-PPD was dissolved in DMAc at room temperature and cooled down to 10 ℃, followed by the addition of TPC to the solution with vigorous stirring under nitrogen purging. Equimolar amounts of Li_2CO_3 were titrated to neutralize the polymerized solution, and HCl was generated as a by-product after polymerization was completed. Washing with water and acetone was repeated several times to obtain CY-PPTA, whose intrinsic viscosity was 5.2 g/dl in 100% H_2SO_4. CY-PPTA solutions in DMAc/LiCl were prepared by vigorous stirring at 60 ℃ for 48 h and the $1-15$ wt% CY-PPTA solutions were prepared by diluting the 15 wt% solution.
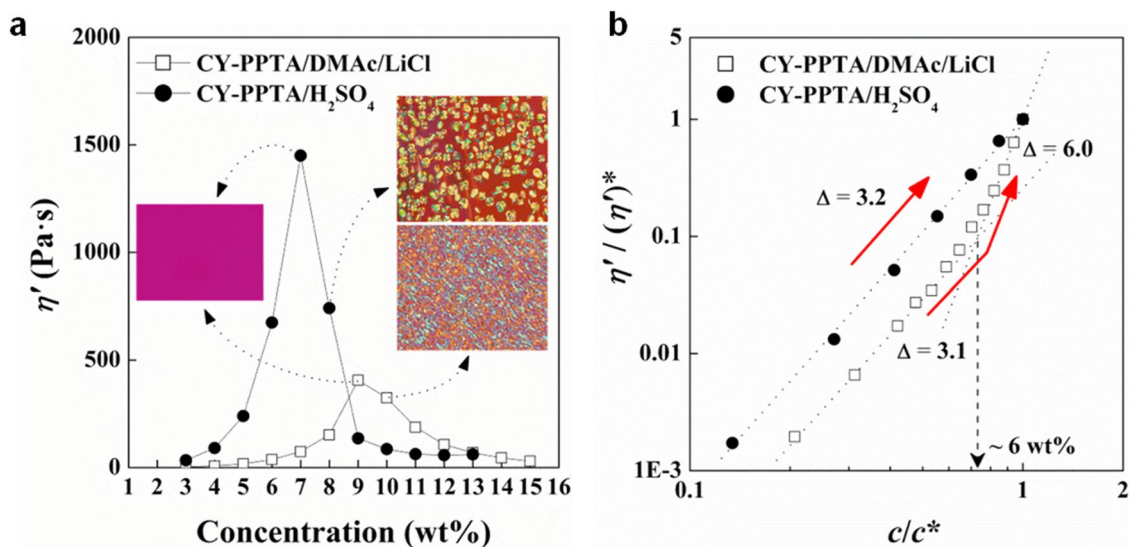

Fig. 1 a Critical concentration (c^*) curves of the CY-PPTA solutions in DMAc/LiCl and H_2SO_4 at a shear rate of 0.05 s^{-1} at 30 °C (inset Figs: polarized optical micrographs at a certain concentration) and b their normalized graphs focusing on the isotropic region below the c^*
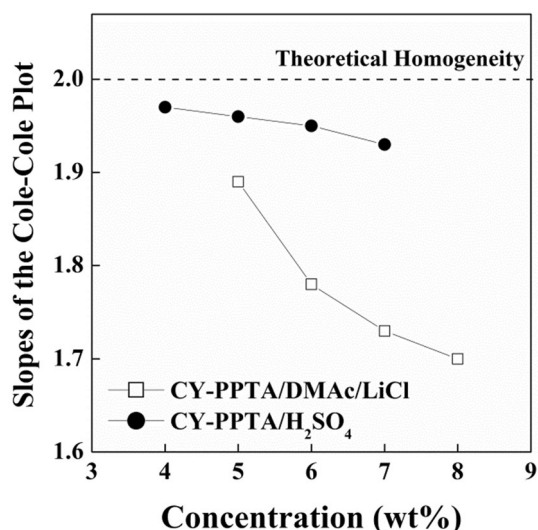
Fig. 2 Variations of the slope on Cole–Cole plots for the CY-PPTA solutions in DMAc/LiCl and H_2SO_4 with increasing solution concentrations

2.2 Characterization

The liquid-crystalline texture was observed using a polarized optical microscope (BX51, Olympus, Japan) equipped with a CCD camera (HFX-11A, Nikon, Japan). The CY-PPTA solution was loaded onto a glass slide, covered with a cover glass, and pressed to form a thin layer. To minimize the evaporation of the solvent during the increase in temperature, the edge of the cover glass was coated with heavy mineral oil.

The rheological properties of CY-PPTA solutions were measured using an Advanced Rheometer 550 (AR-550, TA Instruments, USA). A quartz parallel-plate geometry was used to prevent corrosion by H_2SO_4. The diameter of the upper plate and gap between the plates were 50 and 0.8 mm, respectively. A 5% strain level was used. To ensure the reproducibility of the data, all specimens were pre-sheared prior to the measurement for 1 min at a shear rate of 1 s^{-1} and stabilized for 1 h at a given temperature to eliminate the residual stresses exerted during the gap setting. The edge
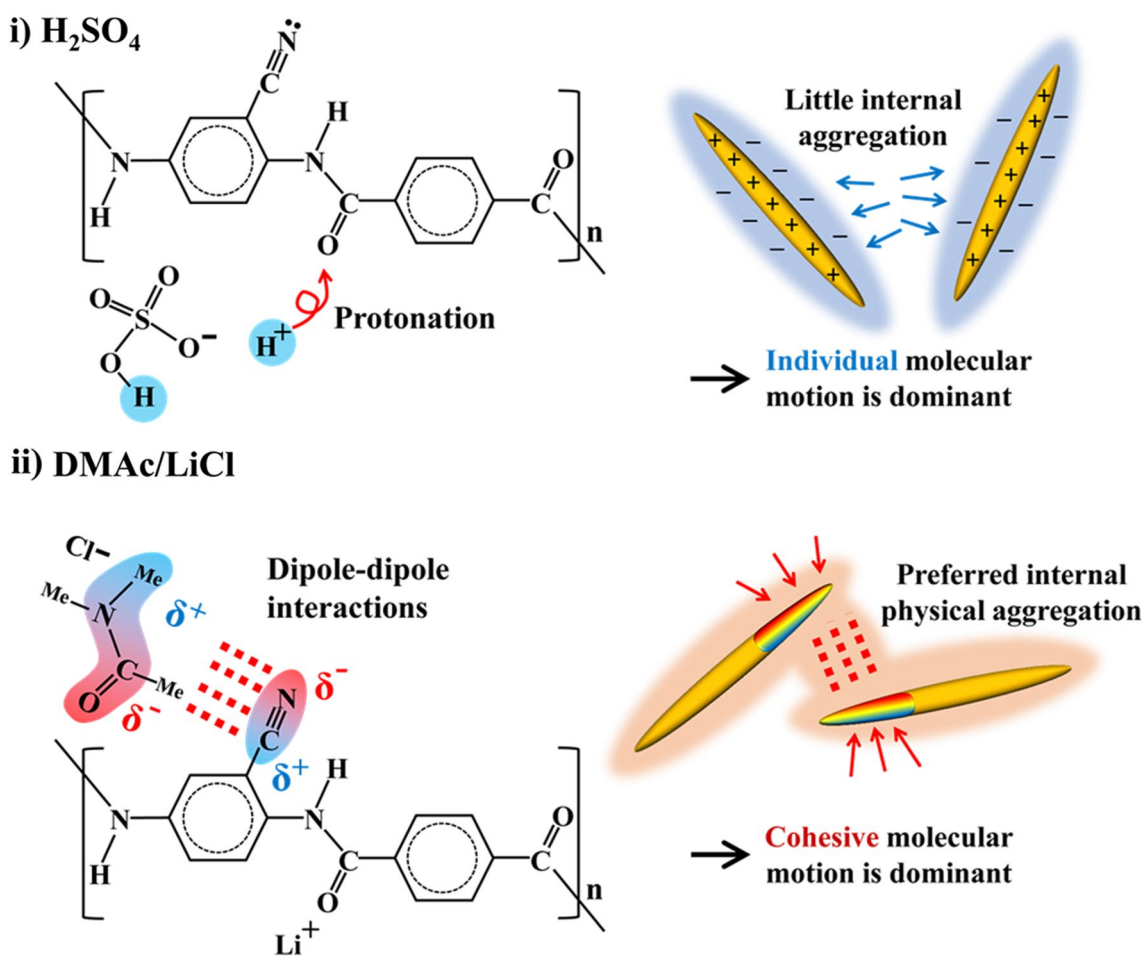
Scheme 1 The proposed solvation process of CY-PPTA molecules in H_2SO_4 and DMAc/LiCl
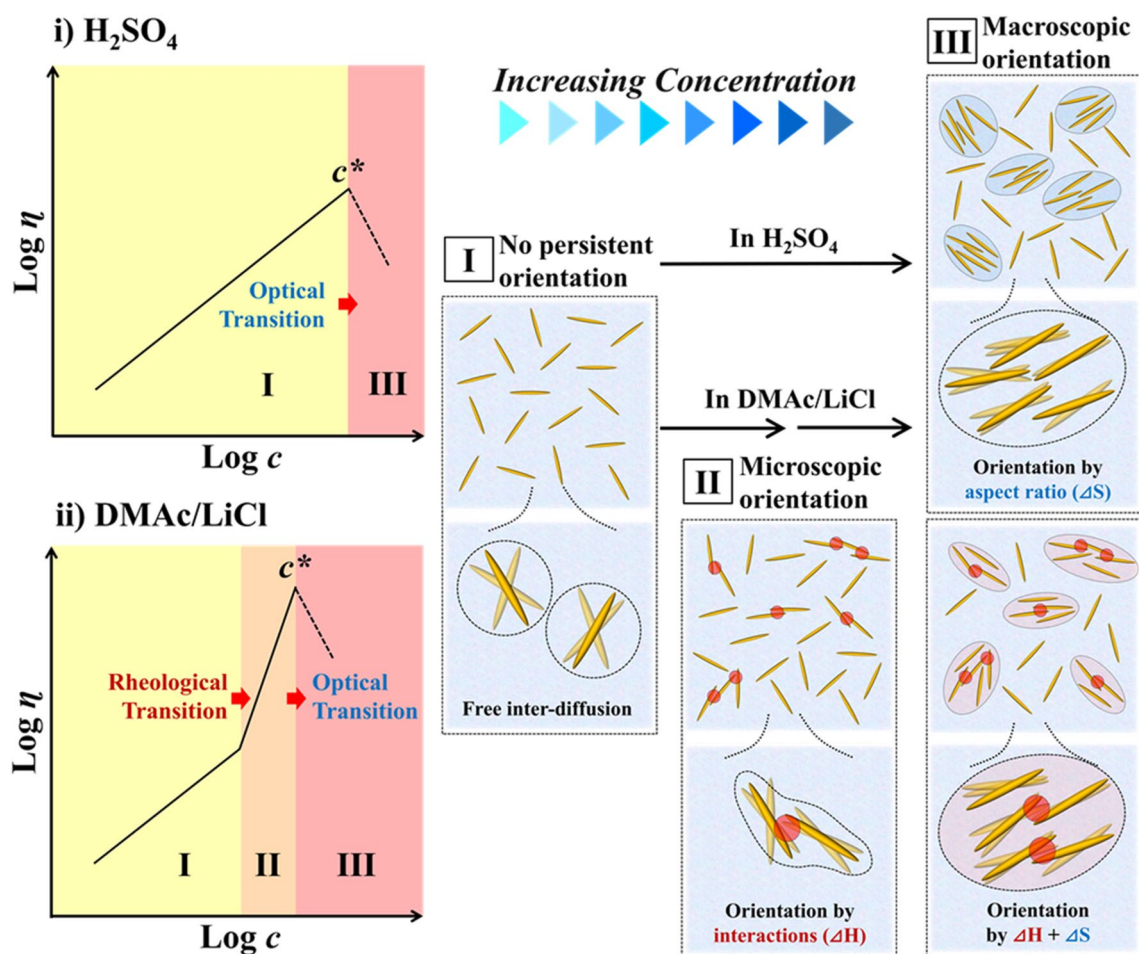
Scheme 2 Schematic of proposed structural ordering behavior of CY-PPTA molecules in H_2SO_4 and DMAc/LiCl with respect to polymer concentration

of the plate was coated with heavy mineral oil to prevent solvent evaporation during the measurements.

3 Results and discussion

Figure 1a shows the variations of the dynamic viscosity (η') with concentration for the CY-PPTA solutions in two different solvent systems at 30 ℃. The c^* curves yield peaks of η' in DMAc/LiCl and H_2SO_4 at 9 and 7 wt%, respectively. In the optical observations (inset Figs of Fig. 1a), while both solution systems exhibit a negligible texture at each c^*, the phase transition occurs beyond the peak, which is attributed to the evolution of the LC domains. Hence, the two solution systems exhibited a similar and typical trend of lyotropic LC phase behavior with increasing CY-PPTA concentration. In the isotropic region below the c^*, however, the concentration dependency of the η' exhibits a different tendency depending on the solvent systems. To further analyze the viscosity–concentration relationship in the isotropic phase,

the normalized curves are plotted in Fig. 1b. In H_2SO_4, the η' increases linearly with a constant slope of 3.2 in the isotropic phase before reaching c^*. In DMAc/LiCl, the power-law exponent of the η' changes drastically from 3.1 to 6.0 in the middle of the isotropic phase at *ca.* 6 wt%. This inflection reveals the evolution of the pseudostructure composed of intermolecular-interacting CY-PPTA molecules, even in the isotropic phase.

Although a similar shoulder behavior below c^* was observed by Aharoni [10, 14], there were some differences between the CY-PPTA system and Aharoni's work. Unlike the reduced slope in the shoulder zone observed by Aharoni, the CY-PPTA solutions in DMAc/LiCl showed the opposite trend; that is, the slope increased. In addition, in the case of Aharoni, small birefringent droplets of the LC domains were observed from the lower end of the shoulder, but the CY-PPTA solutions remained transparent, with negligible development of the LC domains before c^*. Aharoni ascribed this shoulder behavior to the polydispersity of polymers. More specifically, the reduced viscosity slope and presence
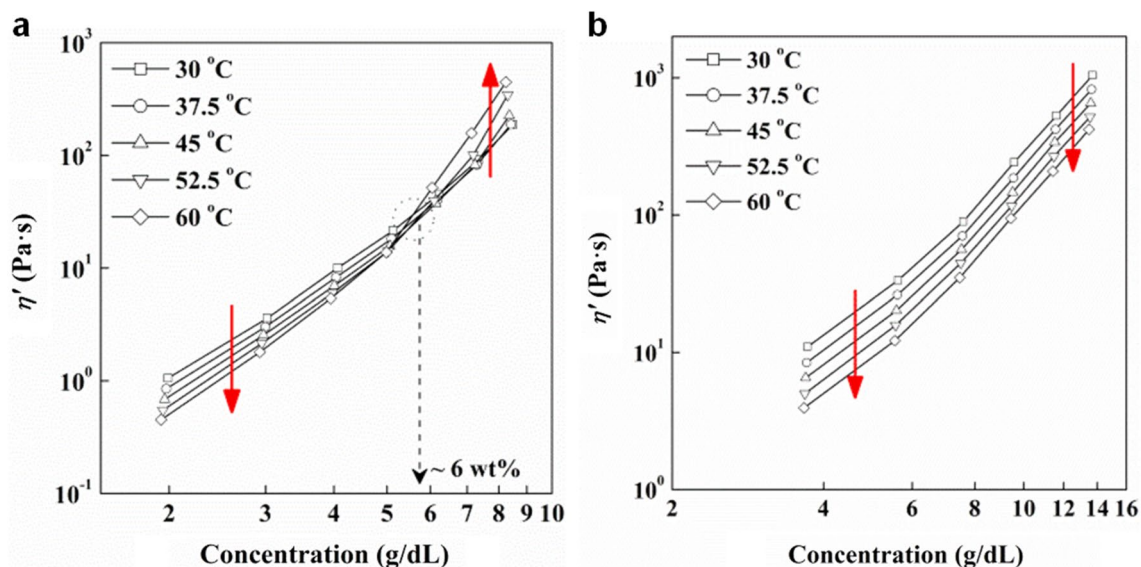
Fig. 3 Temperature dependence of the c^* curves for the CY-PPTA solutions in **a** DMAc/LiCl and **b** H_2SO_4

of LC domains over the shoulder zone were attributed to the earlier molecular orientation of the high-molecular-weight polymers. In the case of CY-PPTA, the exponent change cannot be fully explained by the polydispersity effect alone, because it is affected by the solvent system. This means that the polymer–solvent interactions also play a crucial role in determining the appearance of the shoulder behavior.

Doi et al. calculated that the shear viscosity of rod-like polymers capable of generating a nematic LC phase above c^* changed according to the following equation [11, 15, 16]:

$$\left(\frac{\eta}{\eta^*}\right) = \left(\frac{C}{C^*}\right)^3 \frac{(1-S)^4(1+S)^2(1+2S)(1+\frac{3S}{2})}{(1+\frac{S}{2})^2} \quad (1)$$

in which η and η^* represent the shear viscosity and viscosity at c^*, and S is the orientation parameter. Below c^* where no preferred molecular orientation is present in the solution ($S = 0$), the equation is reduced to the linear dependence of $\eta \sim c^3$. Although the theoretical estimation shows good agreement with the slope of 3.2 in H_2SO_4 within a reasonable
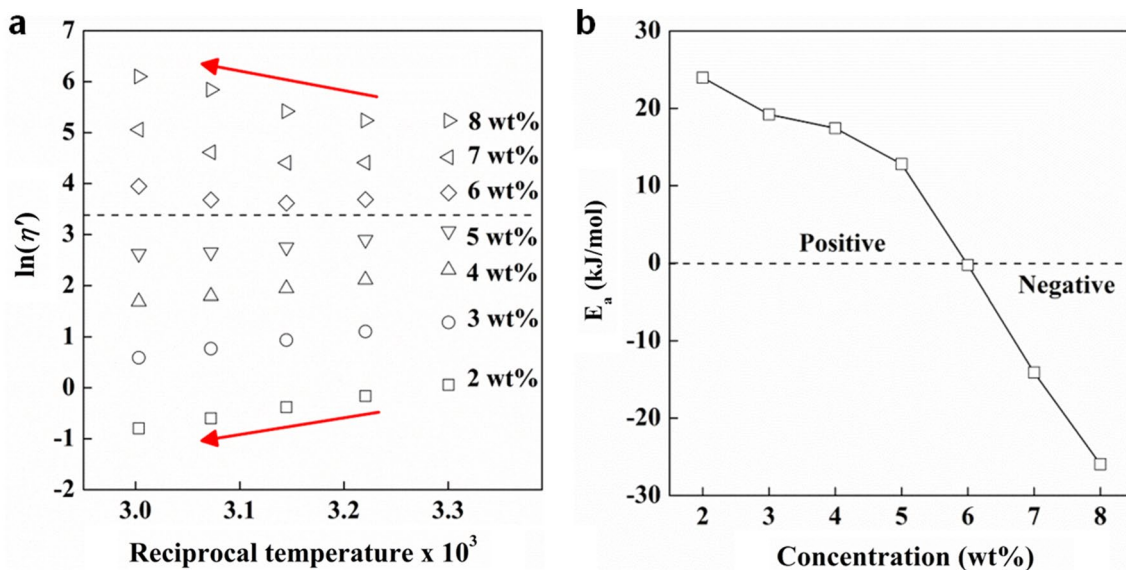

Fig. 4 Arrhenius-type plot of **a** viscosity versus reciprocal temperature and **b** Arrhenius flow activation energy (E_a) as a function of concentration for the CY-PPTA/DMAc/LiCl solutions
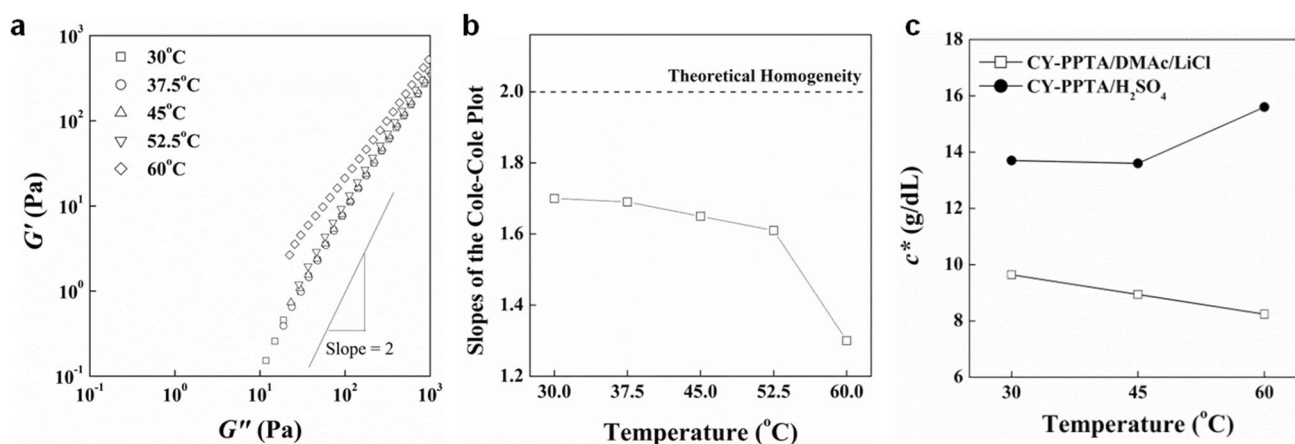
Fig. 5 **a** Modified Cole–Cole plots of the 8 wt% CY-PPTA solution in DMAc/LiCl at various temperatures, **b** temperature-dependent change of initial slopes in the Cole–Cole plot, and **c** the shift of the c^* of the two solution systems with increasing temperature

experimental error range, the slope of 6.0 in the DMAc/LiCl system above 6 wt% deviates significantly from the theoretical value. In theory, it was assumed that there was no specific interaction between the polymer molecules when deriving the equation [17]. However, in real polymeric systems, specific types of intermolecular interactions, such as hydrogen bonding and dipole–dipole interactions, are quite common. Hence, an unrealistic assumption could cause a discrepancy between the experimental and theoretical results for this highly polar polymer solution [8]. In other words, in addition to the polydispersity effect, intermolecular interactions between the CY-PPTA molecules would affect the slope of the viscosity curve in the isotropic phase.

The homogeneity of the CY-PPTA solutions in the two solvent systems was compared with respect to the solution concentration in the isotropic phase. Although the CY-PPTA/DMAc solutions are optically homogeneous below c^*, the deviation of the power-law exponent of the η' curves suggests the presence of the heterogeneous structure. In the plot of the storage modulus (G') versus the loss modulus (G''), the so-called Cole–Cole plot, the initial slope in the terminal zone yields the value of two if the system is absolutely isotropic and homogeneous [18, 19]. Otherwise, the initial slope decreases with increasing heterogeneity because the shear-induced breakup of the internal structures dissipates energy, which is regarded as the loss term. In Fig. 2, the concentration-dependent variations in the initial Cole–Cole slopes are compared for the two solvent systems. The CY-PPTA solutions exhibited better homogeneity (i.e., a higher slope) in the H_2SO_4 system than that in DMAc/LiCl because of their higher solubility in the former solvent [12]. Remarkably, the CY-PPTA/DMAc solutions exhibited a sharp reduction in the slope with increasing concentration, while the CY-PPTA/ H_2SO_4 solutions retained relatively high Cole–Cole slopes above 1.9 at the elevated concentration.

That is, the homogeneity of the CY-PPTA solutions was predominantly dependent on the polymer concentration in the isotropic phase owing to the formation of intermolecular interactions.

At the molecular level, the rheological heterogeneity in the DMAc/LiCl system can be ascertained by predicting the solvation process of CY-PPTA in DMAc/LiCl. A previous study showed that the cyano groups of CY-PPTA molecules generate strong intermolecular dipole–dipole interactions in DMAc/LiCl [13]. Thus, the solvation states of CY-PPTA were quite different in the two solvents, as illustrated in Scheme 1. In H_2SO_4, it is expected that the entire CY-PPTA molecule would be completely solvated because the protonation of H_2SO_4 to every carbonyl group in the amide linkage of CY-PPTA creates a net electrostatic charge on the polymer molecules; thus, they are effectively separated from one another. However, in DMAc/LiCl, the pendant cyano groups generate strong dipole–dipole interactions in the support of highly polar DMAc solvent molecules. These preferred molecular associates would lead to the formation of a physical structure, even in the isotropic phase, which eventually leads to high rheological heterogeneity. However, they are undetectable in optical observations because the size of the associates of the polar groups is much smaller than the wavelength of visible light.

Scheme 2 illustrates the expected molecular behavior of CY-PPTA in two different solvent systems at increasing concentrations. In H_2SO_4, the molecular aggregation of CY-PPTA molecules begins at c^* in the form of LC domains, and this optical transition is predominantly driven by an entropic factor, that is, the anisotropic shape of the molecules, because of the little involvement of the polymer–polymer interactions. However, in DMAc/LiCl, pre-existing microaggregation induced by the dipole–dipole interactions occurs below c^*. That is, enthalpic effects can contribute to
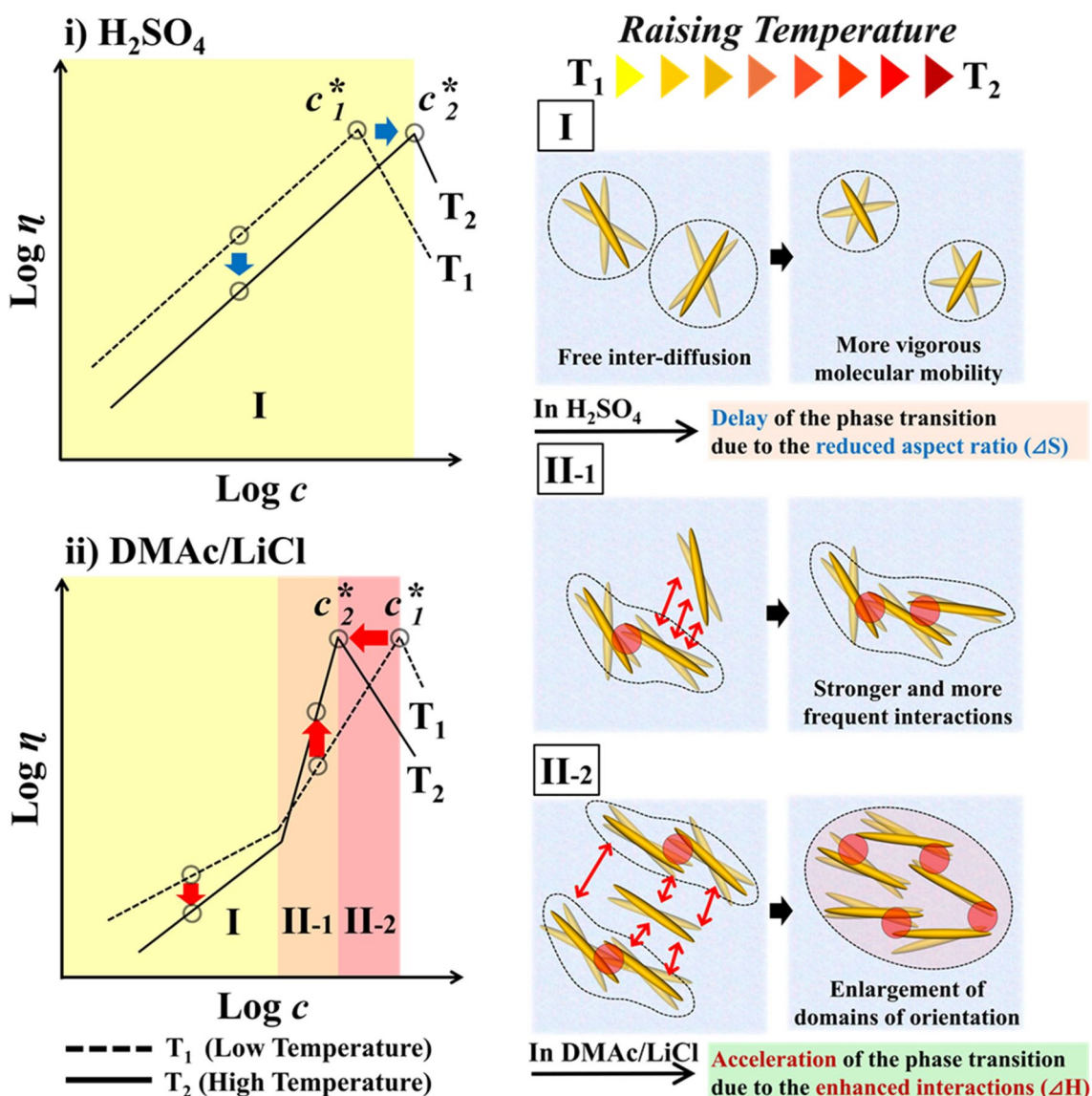
Scheme 3 Schematic of proposed ordering behavior of CY-PPTA molecules with increasing temperature in H_2SO_4 and DMAc/LiCl

pseudostructure formation, even in the isotropic phase of CY-PPTA.

Along with the abnormal transition of the CY-PPTA/DMAc solutions in the isotropic phase, they experienced LCST behavior with increasing temperature. Figure 3a and b compares the temperature-dependent changes in the c^* curves in the two solvent systems (in this case, the concentration is expressed in the volume concentration (g/dL) instead of the weight concentration (wt%) to rule out the influence of the solvent density and to conform with the theoretical expression). Figure 3a shows the c^* curves in the DMAc system, in which the slope change of the η' in the middle of the isotropic region becomes more noticeable with increasing temperature. In contrast, in H_2SO_4, the slope remained almost unchanged irrespective of the

temperature. Furthermore, unlike the monotonous decrease in the η' in H_2SO_4 over the entire concentration range, a more complicated change is observed in DMAc/LiCl. With increasing temperature, while the η' decreases at low concentrations, it increases between the concentrations of 6 wt% and c^*, demonstrating the typical LCST trend [20]. To trace the temperature dependence of the CY-PPTA/DMAc solutions more clearly, it is replotted into the Arrhenius-type plot in Fig. 4a. The slope of the Arrhenius plot indicates the flow activation energy (E_a) [21, 22]. Figure 4b shows that E_a becomes negative above 6 wt%. The negative sign of E_a suggests spontaneous orientation of the molecules upon flow. Hence, the negative E_a is attributable to the presence of pre-organized molecular associates at lower temperatures because the boundary concentration of the sign inversion at

6 wt% agrees well with the concentration showing the slope change at *ca*. 6 wt% (Fig. 1b). Hence, it can be inferred that the presence of a pre-organized molecular orientation brings about spontaneous flow upon increasing the temperature.

The spontaneous molecular orientation in terms of the temperature in the DMAc/LiCl system is closely correlated with the aforementioned rheological heterogeneity. A Cole–Cole plot of the 8 wt% CY-PPTA solution in DMAc/LiCl immediately below $c*$ was obtained to analyze the variation in the heterogeneity with temperature (Fig. 5a). According to the temperature-dependent variation of the Cole–Cole slope (Fig. 5b), the decreased slope clearly confirms the degraded homogeneity of the CY-PPTA solutions with increasing temperature. In other words, the intermolecular interactions induced by the polar cyano groups become stronger as the temperature increases, and accordingly, the pseudo-structure becomes extensive, resulting in LCST behavior. Consequently, as the temperature increased, while $c*$ shifted to a higher concentration in the H_2SO_4 system, it exhibited a downward shift in the DMAc system, indicating the accelerated formation of LC domains (Fig. 5c).

The overall expected molecular behavior with increasing temperature is summarized in Scheme 3 for the two different solvent systems. The monotonous decrease in the η' and the upward shift of the $c*$ in H_2SO_4 are both attributable to the enhanced molecular mobility at an elevated temperature. The resultant reduced aspect ratio (x) of the CY-PPTA molecules at higher temperatures led to a delay in the transition, following the theoretical equation of the inverse proportionality of c^* and x. In DMAc/LiCl, a similar trend was observed at low concentrations. With increasing concentration, however, physical aggregation intensifies at high concentrations. At very high concentrations close to $c*$, the physical aggregations induce an enlargement of the domain size of the molecular orientation and finally leads to the emergence of LC domains.

4 Conclusions

This study revealed that the transparency of the isotropic phase of LC polymers only guarantees the absence of a molecular aggregation larger than the wavelength of visible light. As a supplementary and alternative tool of optics, rheological analysis proved to be efficient in characterizing micro-heterogeneity, which is highly probable in the isotropic phase. The shoulder behavior in the c^* curve was indicative of the preliminary aggregation of LC polymers below c^* in an infinitesimally small size, which is transparent but rheologically heterogeneous. The microheterogeneity of the isotropic phase is closely coupled with the LCST phase behavior. Thus, it is risky to consider an optically isotropic phase as absolutely homogeneous.

Declarations

Conflict of interest The authors declare no conflicts of interest.

References

1. Balbi C, Bianchi E, Ciferri A, Tealdi A, Krigbaum WR (1980) Equilibria of extended-chain polymers exhibiting crystalline and liquid-crystalline phases. J Polym Sci Pol Phys 18:2037–2053
2. Miller DS, Carlton RJ, Mushenheim PC, Abbott NL (2013) Introduction to optical methods for characterizing liquid crystals at interfaces. Langmuir 29:3154–3169
3. Yakacki CM, Saed M, Nair DP, Gong T, Reed SM, Bowman CN (2015) Tailorable and programmable liquid-crystalline elastomers using a two-stage thiol–acrylate reaction. RSC Adv 5:18997–19001
4. Shirai T, Shuai M, Nakamura K, Yamaguchi A, Naka Y, Sasaki T, Clark NA, Le KV (2018) Chiral lyotropic chromonic liquid crystals composed of disodium cromoglycate doped with water-soluble chiral additives. Soft Matter 14:1511–1516
5. Milak S, Zimmer A (2015) Glycerol monooleate liquid crystalline phases used in drug delivery systems. Int J Pharm 478:569–587
6. Dierking I, Al-Zangana S (2017) Lyotropic liquid crystal phases from anisotropic nanomaterials. Nanomaterials 7:305
7. Meeting S, Chester W, Magat EE, Kwolek L, Morgan PW, Morgan W, Kwolek L, Morgan PW, Morgan W, Morgan W, Morgan W, Kwolek L, Morgan PW, Morgan W (1977) Synthesis, anisotropic solutions, and fibers of poly(l,4-benzamide). Macromolecules 10:1390–1396
8. Eom Y, Kim BC (2014) Solubility parameter-based analysis of polyacrylonitrile solutions in N, N-dimethyl formamide and dimethyl sulfoxide. Polymer 55:2570–2577
9. Eom Y, Ju H, Park Y, Chae DW, Jung YM, Kim BC, Chae HG (2020) Effect of dissolution pathways of polyacrylonitrile on the solution homogeneity: Thermodynamic- or kinetic-controlled dissolution. Polymer 205:122697
10. Aharoni SM, Hatfield GR, O'Brien KP (1990) Bending of polyamide rigid rodlike segments. Macromolecules 23:1330–1342
11. Doi M (1981) Molecular dynamics and rheological properties of concentrated solutions of rodlike polymers in isotropic and liquid crystalline phases. J Polym Sci Polym Phys 19:229–243
12. Jung DE, Kim HJ, Chae DW, Kim BC, Eom Y (2022) Rheological and morphological evidence of binary liquid crystalline phases in solutions of an organo-soluble cyano-substituted p-aramid. Polymer 260:125357
13. Jung DE, Eom Y, Kim BC (2019) Enthalpy-driven transition of liquid crystalline textures of poly(2-cyano-p-phenylene terephthalamide) in N, N-dimethyl acetamide/lithium chloride. Macromol Res 27:404–411
14. Aharoni SM (1979) Rigid backbone polymers. 2 Polyisocyanates and their liquid-crystal behavior. Macromolecules 12:94–103
15. Doi M (1980) Rheological properties of rodlike polymers in isotropic and liquid crystalline phases. Ferroelectrics 30:247–254
16. Doi M (1975) Rotational relaxation time of rigid rod-like macromolecule in concentrated solution. J Phys 34:607–611

17. De Gennes PG (1971) Reptation of a polymer chain in the presence of fixed obstacles. J Chem Phys 55:572–579

18. Song J, Choi YH, Kim HJ, Kim H, Eom Y (2023) Control of reinforcing efficiency in thermoplastic polyurethane/aramid nanofiber nanocomposites: rheological and two-dimensional correlation spectroscopic approaches. Eur Polym J 193:112106

19. Kim HJ, Jeong JH, Choi YH, Eom Y (2021) Review on cellulose nanocrystal-reinforced polymer nanocomposites: processing, properties, and rheology. Korea Aust Rheol J 33:165–185

20. Chaudhary G, Ghosh A, Kang JG, Braun PV, Ewoldt RH, Schweizer KS (2021) Linear and nonlinear viscoelasticity of concentrated thermoresponsive microgel suspensions. J Colloid Interface Sci 601:886–898

21. Kim YC, Min H, Hong S, Wang M, Sun H, Park IK, Choi HR, Koo JC, Moon H, Kim KJ, Suhr J, Do Nam J (2017) Multistep cure kinetic model of ultra-thin glass fiber epoxy prepreg exhibiting both autocatalytic and diffusion-controlled regimes under isothermal and dynamic-heating conditions. Korea Aust Rheol J 29:157–162

22. Chen T, Zhang Y, Xu W (2016) Single-molecule nanocatalysis reveals catalytic activation energy of single nanocatalysts. J Am Chem Soc 138:12414–12421